



Metallic Glasses and Glass Forming Melts under External Forces or Reduced Dimension: Molecular Dynamics Simulations

K. Brinkmann, Küchemann, H. Teichler

published in

NIC Symposium 2001, Proceedings,
Horst Rollnik, Dietrich Wolf (Editors),
John von Neumann Institute for Computing, Jülich,
NIC Series, Vol. **9**, ISBN 3-00-009055-X, pp. 233-242, 2002.

© 2002 by John von Neumann Institute for Computing

Permission to make digital or hard copies of portions of this work for personal or classroom use is granted provided that the copies are not made or distributed for profit or commercial advantage and that copies bear this notice and the full citation on the first page. To copy otherwise requires prior specific permission by the publisher mentioned above.

<http://www.fz-juelich.de/nic-series/volume9>

Metallic Glasses and Glass Forming Melts under External Forces or Reduced Dimension: Molecular Dynamics Simulations

K. Brinkmann, K.-B. Küchemann, and H. Teichler

Institut f. Materialphysik
Universität Göttingen, 37073 Göttingen, Germany
E-mail: teichler@umpa06.gwdg.de

Results are reported from molecular dynamics computer simulations for metallic glasses and glass-forming melts under external shear deformations or reduced dimensions. The simulations provide rather unique possibilities to study on the atomic level modifications of the amorphous state of matter under external perturbations. Modelling constant-shear-stress deformations makes visible details of the atomistic mechanisms of plastic deformations of the glasses. Constant-strain-rate processes reveal a deformation induced change of the amorphous structure into a state of easy deformability. This latter state here is ascribed to the interior of the shear bands observed experimentally under ambient temperatures. From the simulations, its properties are characterised in some detail. Local changes of the amorphous state are also studied in the second part of the project, which is concerned with thin films of glass-forming melts and glasses. In particular it is described that for simulated $\text{Ni}_{0.2}\text{Zr}_{0.8}$ - and $\text{Ni}_{0.81}\text{B}_{0.19}$ -films a chemical demixing takes place near the film surface while earlier studies of mid-concentration $\text{Ni}_{0.5}\text{Zr}_{0.5}$ -films revealed in a nm-layer near the surface a significant change of the atomic dynamics by two orders of magnitude without change of the chemical composition.

1 Introduction

Metallic glasses exhibit technologically interesting combinations of properties such as good corrosion resistance, high strength and stiffness at ambient temperatures and high strain-rate superplasticity and workability at elevated temperatures. With regard to the presumed innovative technological perspectives, in particular of the so called 'bulk metallic glasses' developed in the last ten years, strong efforts are made world wide to understand in detail the atomic mechanisms governing the behaviour of this class of materials in order to enlighten the fundamentals for design and control of their properties.

Regarding recent advantages in computing technology — parallel computers on the hardware side, robust algorithms on the software side, and significant improvements in reliably modelling realistic systems — computational approaches play an increasing role in this field, as they can provide more complete and detailed data than often experiments can do for such complex and highly non-linear systems. In accordance with this trend, the present project uses large-scale computer simulations to gain information on the atomic level about the response of glassy materials and their melts to either mechanical external forces or to inhomogeneities like surfaces or interfaces.

In case of mechanical forces, the absence of long range order and of translation symmetry for the glassy state makes inapplicable the standard models of plastic response developed for crystalline solids. Important contributions to modelling the plastic behaviour of glasses have been provided in the past, e.g., by Spaepen¹, who described the plastic deformation as arising from single atom jumps, by Argon², where the plastic response is

viewed to be due to reorientation of clusters containing a larger number of atoms, and Tomida and Egami³, promoting the bond-exchange mechanism. But there remain fundamental questions, particularly regarding the relationship of these models to the present successful approaches in describing diffusive matter transport and relaxation dynamics of metallic glasses (for some details see, e.g.,⁴).

The report communicates results from molecular dynamics (MD) simulations for a three dimensional model amorphous solid concerning its response against shear deformations (for further details, see⁵). The study is aimed at elucidating to which extend the plastic response is carried by the original, relaxed amorphous state and to which extend state changes take place under deformations towards a mobile configuration of the glass. Local state changes of related type are the topic of the second part of the project, which is concerned with effects of spatial inhomogeneities, like free surfaces, on the local state in highly viscous liquids and glasses.

2 Dynamics of Metallic Glasses under Shear Deformations

2.1 Simulations

Modelling of the behaviour of a glassy system under shear was carried out for a system adapted to $\text{Ni}_{0.5}\text{Zr}_{0.5}$. The latter is well known as a glass forming metallic system from experiment and MD simulations. Details of the applied model can be found in the literature⁶.

In the present simulations a medium size system was considered containing an ensemble of 5184 atoms subjected to periodic boundary conditions. The MD modelling was carried out with the TABB code⁷, a simulation program optimised for use on parallel machines with shared memory conditions. It makes use of dynamical domain decomposition with distribution of the atomic objects to the domains such that communications take place between adjacent domains only, where each domain means one node on the hardware side. The distribution of atoms takes care of equal computation load for each node and can be refreshed with preselected frequency.

Two different deformation processes have been considered in the simulations: deformations under constant-shear-stress and deformations under constant-shear-strain rate. Constant-shear-strain simulations are carried out at three deformation rates ($\dot{\epsilon} = 0.013 \text{ ns}^{-1}$, 0.035 ns^{-1} , and 0.13 ns^{-1}) each at two temperatures (1000 K and 810 K). Deformation under constant-shear-stress was modelled for 6 stress values (ranging from 200 to 1200 MPa) at the two mentioned temperatures. In order to study the macroscopic dynamics of the system under realistic loading conditions, the simulations covered time windows of 40 ns, each corresponding to $2 \cdot 10^7$ MD integration steps of the system with its more than 15,000 degrees of freedom.

Additional simulation runs were used for preparing well-relaxed initial configurations of the system, including long-time runs over more than 100 ns, for verification whether stationary dynamics already are reached during the processes, for analysing the behaviour under time-dependent loading conditions, and for studying the relaxation and recovery behaviour after deformations.

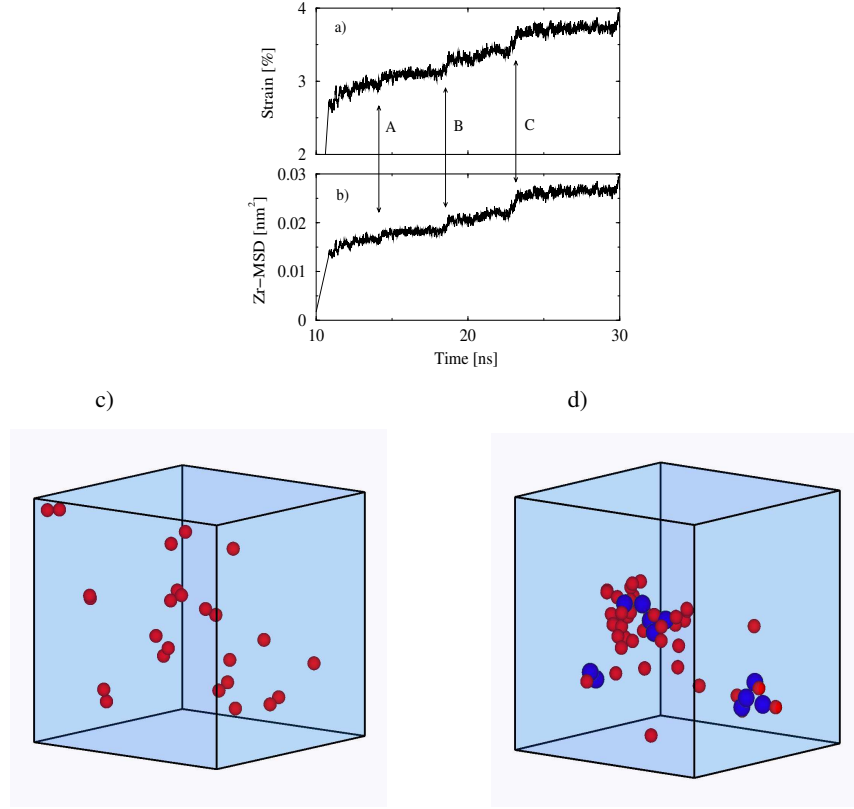


Figure 1. a) Strain evolution with time during loading with constant-shear-stress $\sigma = 1150$ MPa. b) Mean square displacements (MSD) of Zr-atoms versus time for the simulation depicted in a). c) Drawing of the significantly moved atoms in the simulation cell for a time window between jumps marked A and B. d) The same as part c) but for a time window including the jump marked C.

2.2 Results of Constant-Shear-Stress Simulations

For demonstrating our observations during constant-shear-stress simulations, Fig. 1a displays the results of loading the system with 1150 MPa at 810 K. Displayed is the shear strain in the system under constant stress as function of time, the creep curve. The individual events of the plastic shear deformation are visible in the creep curve by peaks and jumps. Comparison of this creep curve with the mean square displacements of Zr-atoms (Fig. 1b) reveals a strong correlation between the macroscopic (shear) strain and the displacements of the Zr atoms, which form the rigid matrix in the considered binary amorphous structure.

Apparently there are two modes of deformation: jump-like transitions denoted in Fig. 1a and 1b by A to C, and a continuous creep-like behaviour between these events. For the jump C, Fig. 1d presents the atoms that carry out significant displacements during this jump. Obviously, the atoms taking place in this jump are heterogeneously distributed in space and form a loose, local cluster, a 'mobile spot'. For comparison, Fig. 1c presents

the atoms that carry out significant movements in the time interval between the jumps A and B. Their distribution is rather diluted in space. A closer analysis shows that the underlying atomic dynamics in this latter creep-like regime can be interpreted as a sequence of individual chain processes, during each of which a chain of atoms, embedded into a more rigid matrix of host material, collectively carries out a transition towards a more favourable configuration. There is evidence that the mobile spots mean local avalanches consisting of a number of such chain processes, similar as discussed by Teichler⁴ as local relaxation processes of the glassy state during aging.

In addition to these descriptive results, the simulated creep curves can be used to estimate the activation volume for creep under constant stress. According to Spaepen¹ and Argon², under stationary creep there holds the relationship between strain rate $\dot{\epsilon}$, shear stress σ , and temperature T , with activation volume Ω , namely $\dot{\epsilon} \sim \sinh(\sigma\Omega/k_B T)$. Analysing simulated strain rates obtained under varying shear stress and temperature yields an activation volume of $7 - 8 \cdot 10^{-29} \text{ m}^3$, corresponding to approximately 5 atomic volumina, in good agreement with experimental estimates⁸.

2.3 Results of Constant-Shear-Strain Rate Simulations

As a typical example, Fig. 2a displays the stress-strain curve obtained from simulations under constant-strain-rate conditions at nominal 1000 K with a deformation rate of 13 % per ns. The stress-strain curve displays a well-developed yield point after initial linear, elastic increase and then turns into a stationary mode. Our results are qualitatively and quantitatively in good agreement with very recent experimental findings at massive glasses under constant-strain-rate deformations⁹.

The observations have to be considered as a clear indication for a strain induced transition of the glass from its initial rigid configuration into a state of easy deformation under constant load. The transition clearly is demonstrated by Fig. 2b. There simulated constant-stress deformation curves are shown of two different pre-deformation states of the system, one from the initial linear-elastic regime and one from the easy-deformation regime beyond the yield point. While the former remains stable under the applied load of 664 MPa,

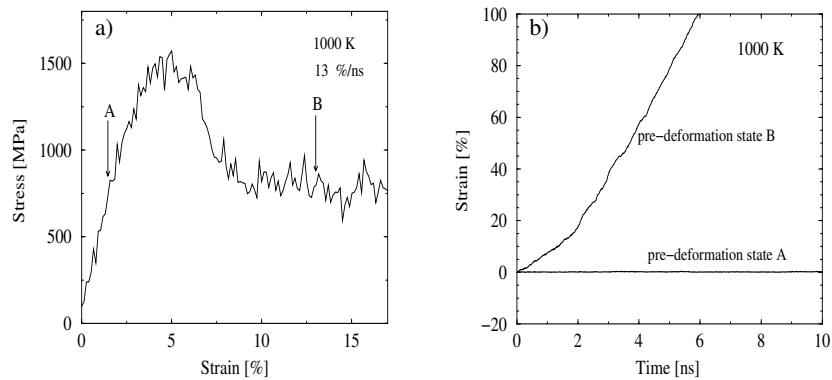


Figure 2. a) Stress-strain-curve for the simulation parameters $\dot{\epsilon} = 13\%/ns$ and $T = 1000 \text{ K}$. b) Creep curves of pre-deformed configurations. The stress in both cases is $\sigma = 664 \text{ MPa}$.

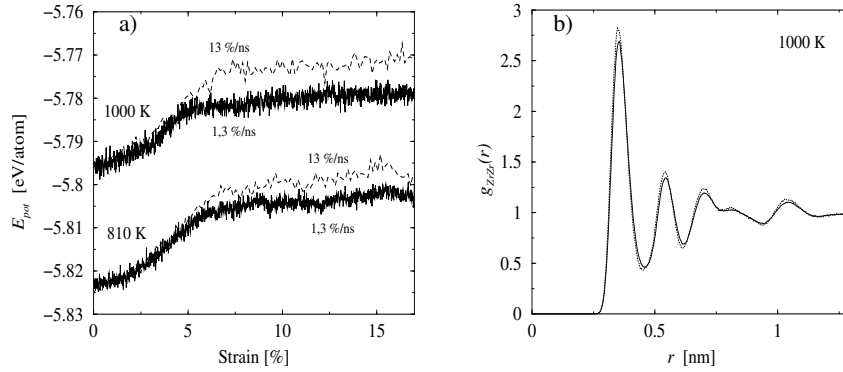


Figure 3. a) Potential energy E_{pot} during the deformation with constant-strain-rate. b) Comparison of radial distribution functions for the Zr-subsystem belonging to two different states of the system: undeformed state (dotted) and easy-deformation state (line) for the stress-strain curve with $\dot{\epsilon} = 13$ %/ns at $T = 1000$ K depicted in Fig. 2a.

the latter shows marked creep under the same conditions and reflects the transition of the system into the deformation-induced easy-deformation state. Similar observations have been obtained at lower strain rates as well as at 810 K.

Our computer studies allow to characterise on the atomic level the properties of the easy-deformation state. Compared to the initial relaxed glassy state, the easy-deformation state shows much higher atomic dynamics, visible in the decay time of the structural α -decay, an increased inner energy of the system (see Fig. 3a), and an increased Wendt-Abraham parameter. The latter means a compact way to measure changes in the radial distribution (comp. Fig. 3b) of atoms and thus in the structure of the system. The observed increased parameters are characteristic for undercooled melts at higher temperatures. Hence, although the atomic vibrations in the deformed system correspond to the temperature of 1000 K, the mentioned global parameters refer to a structure of the system at higher temperature.

2.4 Discussion of the Shear Deformation Results

For metallic glasses it is known that deformation under loading takes place in two different ways, depending on temperature and strength of load: at high temperatures and low loads homogeneous deformations are found, at lower temperatures and higher loads deformation shows a heterogeneous behaviour. The heterogeneous deformation mode is characterised by the formation of planar shear bands of easily deformable material.

Our simulations are carried out well in the temperature regime for which homogeneity is expected. We observe, nevertheless, two distinct modes of deformation in our model system. This fact deserves some discussion. It seems to be related to the large stress and strain rates accessible to computer simulations. According to our impression, the critical quantity is the ratio of energy increase in the system due to plastic deformation compared to the energy dissipation through the structure. The latter depends on the state of the system and should be larger in high-energy configurations. Steady-state deformation demands that both energy contributions are outbalanced. A further increase of the deformation rate

by additional loading leads to an increase of energy in the system and thus automatically turns the system into a state of reduced stiffness but larger energy dissipation. It may be a question of details whether for the larger load a new point of stationarity is obtained or whether an instability takes place.

According to this picture, the easy-deformation state found in the simulated constant-strain-rate processes corresponds to a high-strain-rate structure, that means to the interior of a shear band rather than to the experimental state of homogeneous deformation. The experimentally observed heterogeneous deformation thus means a local transition into the here described 'flow state'. As indicated in the preceding section, the computer simulations allow to identify the microscopic properties of this flow-state of glassy matter and to distinguish it from the relaxed state of the glass in a much more detailed way than it can be expected from experiments.

3 Glasses and Glass Forming Melts at Reduced Dimension

3.1 Simulated $\text{Ni}_{0.5}\text{Zr}_{0.5}$ -Films with Free Surfaces

In a preceding study^{10,11} we had shown by MD simulations that a change of state takes place close to free surfaces of amorphous and liquid $\text{Ni}_{0.5}\text{Zr}_{0.5}$ -films. This change is visible in the atomic dynamics, e.g., in the local diffusion coefficients or local 'hopping rates' (the latter being measured in terms of the life time of the nearest-neighbour relationship). While in the interior of the film the bulk values of the diffusion coefficients are found, the diffusion increases continuously by more than two orders of magnitude in a surface layer of about 1 nm thickness when approaching the film surface. This behaviour has some resemblance to the phenomenon of premelting known at (110) surfaces of some fcc metals. There is, however, the particular difference that in case of premelting an additional inner interface is found while in the amorphous film — and in simulated films of highly viscous liquids — the change takes place continuously. According to these findings, significant changes of the properties of the glassy state are expected in case of reduced dimension, that means once the extension of the glassy material in one dimension is comparable or less than twice the surface layer thickness. It is the objective of the present studies to investigate which changes of the sketched phenomena are to be expected once the chemical composition of the film or the chemical nature of the constituents are modified.

3.2 Simulated $\text{Ni}_{0.2}\text{Zr}_{0.8}$ - and $\text{Ni}_{0.81}\text{B}_{0.19}$ -Films with Free Surfaces

MD simulations for $\text{Ni}_{0.2}\text{Zr}_{0.8}$ - and $\text{Ni}_{0.81}\text{B}_{0.19}$ -films revealed a significantly different behaviour of these materials compared to $\text{Ni}_{0.5}\text{Zr}_{0.5}$. Both materials are characterized by the fact that there is a fraction of about 20 % of smaller atoms dispersed in an amorphous matrix of larger atoms. For both systems, simulated annealing of a film of finite thickness revealed similar features: During annealing, in the interior of the film there takes place an enrichment of the smaller atomic species while at the surface a pure layer of the larger atoms is formed. A particular example of this process is shown in Fig. 4. — The corresponding MD simulations on the Cray T3E of the NIC at Jülich have been carried out by use of the TABB-code addressed in section 2.1.

For the Ni-B system, the freshly formed surface layer of the larger Ni-atoms was removed during the simulations a couple of times, yielding a series of systems with slightly

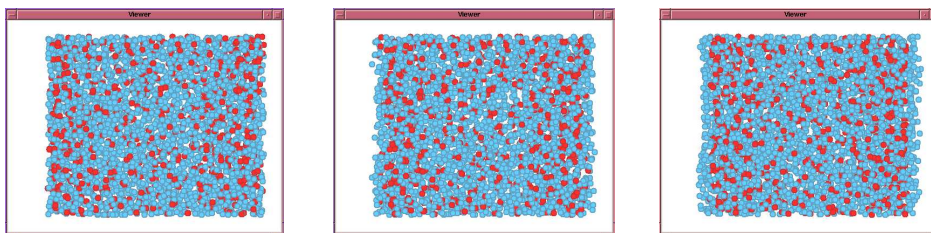


Figure 4. Segregation of Ni in a Ni-B-film: left: start of the simulation, middle: segregation of Ni after 100 ps, right: intermixture in the interior of the sample after 3 ns.

decreasing Ni- and increasing B-content. Under annealing, in each case the freshly formed mixed Ni-B-surface relaxed into a pure Ni-surface with further increase of the B-content in the interior. These observations indicate that — apparently — formation of the larger atoms surface layer is a particular property of the surface structure for the considered glassy states. By formation of this structure, the density of energetically favourable NiB-bonds (resp. ZrNi-bonds in the Ni-Zr system) is increased on account of a loss of entropy of mixing in the surface sheet.

It is to be expected that in the Ni-Zr-system the demixing tendency near the surface decreases with decreasing Zr-concentration of the melt, leading to a homogeneous chemical composition for mid-concentration films. The details of this process are, however, not yet known.

3.3 Sandwich Structures of Amorphous NiZr and Crystalline Zr

While the preceding section considers glassy and viscous liquid films with free surfaces, the present section reports some results obtained for viscous liquid Ni-Zr films between crystalline Zr-walls. During annealing of such sandwich structures, by either growth of the crystalline Zr-structure or partial dissolution of the crystal under growth of the melt, the composition of the melt is adjusted to the concentration of the liquidus curve describing the thermodynamic equilibrium between the highly viscous liquid and the Zr-crystal at the considered annealing temperature. — Fig. 5 demonstrates for a $\text{Ni}_{0.2}\text{Zr}_{0.8}$ -melt between crystalline Zr-walls the broadening of the crystalline layers under Ni-enrichment of the melt obtained from MD simulations for nominally 1250 K.

Due to the temperature dependence of the liquidus concentration, a temperature change demands a change of the equilibrium composition of the melt and hence crystal growth or dissolution. With regard to this, a series of relaxations of the system under successive cooling was carried out, yielding a stepwise increase of the Ni-content in the melt. On the other hand, a series of relaxations under stepwise increase of the temperature gave a series of stepwise decrease of the Ni-content in the melt. It is to be expected that the equilibrium liquidus concentration just lies between the Ni-concentrations from cooling and from heating and that the equilibrium concentration thus can be estimated from these simulations. The here sketched simulations open the way to study in detail on the atomistic level the structure and further properties of the crystal-melt interface. In the following we shall exploit, however, a different aspect of these simulations, which is related to the question of stability of the melt against concentration fluctuations.

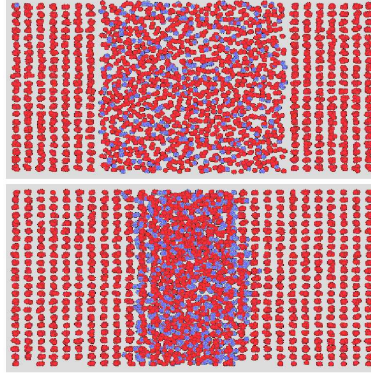


Figure 5. Segregation of crystalline Zr from a $\text{Ni}_{0.2}\text{Zr}_{0.8}$ -melt embedded between Zr-walls in MD simulations corresponding to 1250 K. Top: starting configuration, bottom: configuration found after nominal 25 ns of aging time.

3.4 Discussion of the Simulations of Glass-Forming Melts with Reduced Dimension

In Section 3.3 we described MD simulations for a sandwich structure of liquid $\text{Ni}_{1-x}\text{Zr}_x$ and crystalline Zr. The resulting continuous shift of the equilibrium Ni-concentration with temperature, as sketched in Fig. 6, indicates for Gibbs thermodynamic potential of the melt in the considered concentration regime a convex curvature with composition. According to this finding the NiZr-melt in this regime will be stable against composition fluctuations without any tendency for demixing.

With this knowledge we now shall consider the simulations described in Section 3.2. There we found near the surface, e.g., of the $\text{Ni}_{0.2}\text{Zr}_{0.8}$ -film a local change in composition yielding a pure Zr layer on the film accompanied by an enrichment in the interior. Regarding the just mentioned results of Section 3.3, a volume instability promoting chemical demixing not seems plausible. Thus, there remains the alternative that the driving force

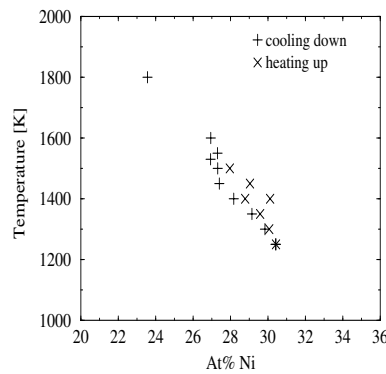


Figure 6. Temperature dependence of the Ni-concentration for a Ni-Zr-melt sandwiched between crystalline walls.

for the observed surface-demixing lies in the surface itself. Accordingly, the concentration profile near the surface should reflect the way the system balances the competition between the preferred surface structure and the volume stability of the melt. — The observations for the Ni-B-melts display a similar behaviour and thus give support to the assumption that these findings are not limited to the NiZr-system but reflect a more general tendency.

Combining the here considered phenomena with the results discussed in Section 3.1 for mid-concentration melts leads to the conclusion that surfaces of the highly viscous melts may give rise to changes in the amorphous structure, yielding a change either in the mobility and atomic dynamics near the surface or in the chemical composition and dynamics. For the low-concentration case, the observed demixing reflects that the composition couples to the surface in this case. In the mid-concentration case, the increased atomic mobility without chemical demixing indicates, however, the existence of an additional hidden parameter in the amorphous structure which governs this mobility and which couples to the surface^{10,11}.

4 Concluding Remarks

The above described MD simulations on highly viscous, glass-forming melts are concerned, in essence, with the question of modulations of the amorphous viscous state. The first part concerns changes of the state under mechanical shear deformations. Regarding this, the provided results demonstrate in case of the creep-curve, Section 2.2, the relaxation dynamics of the equilibrated viscous state under loading. Beyond this, the constant-strain deformations in Section 2.3 describe a change of the amorphous state towards a state of easy deformability. Analysis regarding its energy and Wendt-Abraham parameter revealed some of the properties of this new state, indicating that its structure is similar to that of the equilibrium viscous states at higher temperatures.

The MD simulations^{10,11} had shown that a change of state takes place close to free surfaces of amorphous and liquid Ni_{0.5}Zr_{0.5}-films. This change was visible in the atomic dynamics, e.g., in the local diffusion coefficients and local 'hopping rates'. This change of state was described in terms of a hidden parameter of the amorphous structure^{10,11}. The present MD simulations show that the surface modifies the chemical composition in case of Ni-poor Ni-Zr-films (and Ni_{0.81}B_{0.19} films). They give a clear picture of the chemical demixing near surfaces and makes obvious that the phenomena in the mid-concentration Ni-Zr-film are rather different from the case of chemical demixing. — Regarding the here sketched modifications of the highly viscous liquid — or glassy — state of matter, computational physics, in particular MD simulations, seem to offer rather unique possibilities to study the phenomena in much more detail than accessible to present experiments. The variety of results may encourage, however, the design of appropriate experimental studies.

Acknowledgements

The authors acknowledge support of this study by the NIC by providing the necessary CPU time on the Cray T3E. Financial support is acknowledged from the DFG in the new SPP "Phasenumwandlungen in mehrkomponentigen Schmelzen" and by the Sonderforschungsbereich 345 der DFG "Festkörper weit weg vom Gleichgewicht".

References

1. F. Spaepen, *Acta Met.* **25**, 407 (1977).
2. A. S. Argon, *Acta Metall.* **27**, 47 (1979).
3. T. Tomida and T. Egami, *Phys. Rev. B* **48**, 3048 (1993).
4. H. Teichler, *J. Non-Cryst. Solids* **293-295**, 339 (2001); H. Teichler, *J. Non-Cryst. Solids*, submitted.
5. K. Brinkmann, Diploma Thesis, Univ. Göttingen (2000).
6. H. Teichler, *Phys. Rev. B* **59**, 8473 (1999); H. Teichler, *Phys. Rev. Lett.* **76**, 62 (1996); A. B. Mutiara and H. Teichler, *Phys. Rev. E* **64**, 046133 (2001).
7. B. Böldeker and H. Teichler, in: *Molecular Dynamics on Parallel Computers* (edited by: R. Esser, D. Grassberger, J. Grotendorst and M. Lewerenz), World Scientific 2000, pp 199-210.
8. A. I. Taub, *Scr. Met.* **17**, 873 (1983).
9. H. Kato and Y. Kawamura and A. Inoue and H.S. Chen, *Appl. Phys. Lett.* **73**, 3665 (1998).
10. B. Böldeker, Dissertation, Univ. Göttingen (1999).
11. B. Böldeker and H. Teichler, *Phys. Rev. E* **59**, 1948 (1999).